# State of Gelation of Fully Conjugated Conducting Gels. Gel Fraction, Swelling, and Nuclear Magnetic Relaxation

**Annie Viallat***

*Laboratoire de spectrométrie physique, Université J. Fourier, CNRS (UMR C5588), BP87, 38402 Saint Martin d'Hères Cedex, France*

**Brigitte Pépin-Donat**

*CEA/Département de recherche fondamentale sur la matière condensée, SI3M Laboratoire de physique des métaux organiques, CENG 17 av. des Martyrs, 38054 Grenoble Cedex 9, France*

*Received December 27, 1996; Revised Manuscript Received April 29, 1997*[⊗]

ABSTRACT: Statistical properties of well-defined fully conjugated poly(3-octylthiophene) (POT) gels are explored above glass transition and fusion temperatures by varying the cross-link functionality, $f$, and the cross-link concentration, $R_i$. Four series of gels are prepared using four different cross-linking agents. The state of gel connectivity, characterized by the gel fraction is found to depend on the distance to the gelation threshold, $\epsilon$, expressed within a mean-field percolation approach. In the range of explored cross-link densities, $^1$H NMR and swelling experiments reveal that the active structural strands of both dry and swollen gels are the linear chain segments defined by adjacent cross-links. These segments are disengaged from one another in swollen gels. The two variables, chain segment contour length and $\epsilon$, are functions of the product $fR_i$. This parameter is the relevant variable for the description of POT gel structures: master curves of the quantities gel fraction, swelling ratio, and $^1$H transverse relaxation rate are obtained versus $fR_i$.

## I. Introduction

During the past 15 years novel conducting polymers have been designed which present well-defined structures and new properties. In particular, conjugated polymers fusible and soluble in common organic solvents have been synthesized with the aim of improving their processability. Within the same period, electronic properties of these quasi one-dimensional polymer systems have been extensively studied. The conduction process is generally governed by hopping (except in particularly well-ordered structures[1−4]). Intra- and interchain hopping processes may occur. Hence, the resultant macroscopic conductivity depends both on the polymer chains structure and on their three-dimensional solid-state organization. For instance, the conductivity of regioregular poly(alkylthiophenes), which is much higher than that of statistical poly(alkylthiophenes) is not only due to a higher conjugation along the chains but also to an optimized 3D solid-state statistical structure.[5] This point is of importance since polymer systems cannot be fully ordered and generally present complex statistical organizations which involve entangled crystalline and amorphous structures and which depend on the conditions of preparation of the materials.

Contrary to conducting linear chains, conducting gels have not been extensively studied. Gelation of polymer solutions (especially of polyaniline) devoted to fiber or film preparation has been generally considered as a major inconvenience,[6−10] and it is only recently that the interest for conductive gels of polyaniline[11−13] and of poly(alkylthiophenes)[14−29] has grown. In most cases, the nature of cross-links of conducting gels is not well-defined and is even not determined. To our knowledge, the studies of well-defined conducting gels reported in the literature have concerned only two series. The first series, prepared by copolymerization of 3-*n*-octylthiophene with 1,6-di-3-thienylhexane,[30] do not exhibit fully conjugated cross-links. The second series concern fully conjugated polybenzal (m-directing)[31] gels; these do not exhibit significant swelling and have so far not been doped. However, conducting gels are expected to have a great physical interest since they should present an unusual combination of properties:[32] mechanical properties like rubber elasticity and ability of swelling in a good solvent as well as specific transport properties due to the existence of a 3D connected network[33] and to a modulation of the crystalline structure by the presence of cross-links. This combination may lead to possible electromechanical effects.

These properties depend on the statistical topological structure of the gels. More precisely, it is now well-known that the entropy reduction which accompanies the creation of topological constraints upon polymerization and gelation induces a microscopic statistical structure in polymer media. This structure depends on the topology (functionality, chain length between cross-links, loops, dangling chains, entanglements) and on the state of connectivity of the network. It is characterized by a typical chain segment associated with the average mesh size of the network. Furthermore, polymer chains undergo large conformational fluctuations above glass transition temperature. The understanding of the physical properties of polymer networks therefore also requires the description of the probability distribution of end-to-end vectors of gel chain segments. Their collective motions are known to govern the mechanical behavior of the gels.

It is therefore of great interest to synthesize networks with a controlled and reproducible structure. We have prepared gels of poly(3-*n*-octylthiophene) (POT) with well-defined fully conjugated cross-links (trithienylbenzenes)[34,35] and different cross-link densities. It has been already shown that the transport properties[36] of these networks in the doped state depend on the cross-link density.

[⊗] Abstract published in *Advance ACS Abstracts,* July 15, 1997.

S0024-9297(96)01909-2 CCC: $14.00 

This work deals with statistical structural properties of POT gels above glass transition temperature and chain segments melting temperature. Our purpose is to show that the method of synthesis of these gels leads to the formation of reproducible networks whose stastistical properties and structure can be quantitatively studied. More precisely, our objective is to define a variable suitable to predict any physical state of gelation of POT gels (such a variable must combine the parameters concentration and functionality of cross-links). Then, we will show the validity of our approach by establishing master curves of variations of the relevant physical quantities like the gel fraction, the swelling ratio, and the NMR transverse relaxation rate. The understanding of the observed laws of variations will then allow one to characterize the typical segments of a network and to describe its mechanisms of deformation.

The paper is organized as follows. The experimental approach is detailed in section II. The theoretical framework of description is presented in section III. The standard description of gels is evoked, and the model of percolation is briefly recalled. A variable of gelation is proposed. The gel behavior is first explored from the observation of the gel fraction (section IV). The physical state of gels isotropically deformed by a swelling mechanism of chain segments induced by a good solvent is investigated in section V. The state of molecular deformation in dry networks is considered in section VI from a standard NMR approach, based on the observation of the relaxation rate of the transverse magnetization of $^1$H spins located on polymer chains.

## II. Experimental Section

Four trithienylbenzenes have been prepared, characterized,[34] and copolymerized (oxidative polymerization via $FeCl_3$) in chloroform with 3-*n*-octylthiophene (Figure 1). The synthesis has already been described.[34,35] The four series of gels, prepared by using the four different trithienylbenzenes, 1,3,5-tri-2′-thienylbenzene, 1,3,5-tri-3′-thienylbenzene, 1,2,4-tri-2′-thienylbenzene, and 1,2,4-tri-3′-thienylbenzene, are referenced as **1**, **2**, **3**, and **4**, respectively. Their theoretical functionality, *f*, is either 3 (series **1** and **3**) or 6 (series **2** and **4**). Various networks have been made for each series by varying the initial molar fraction of the trithienylbenzene moiety, $R_i$. IR spectroscopy experiments[34] performed on a sample of series **1**, whose reactive groups of cross-links had been deuterated, had shown that these groups had all reacted with 3-*n*-octylthiophene (within the experimental error of the order of 3%).

The reactive medium is poured in methanol where dedoping of the conductive species occurs. Systems prepared with very small fractions $R_i < R_{ic}$ are totally soluble in chloroform and form a sol made of finite size clusters. Systems prepared with higher fractions $R_i > R_{ic}$ exhibit an insoluble macroscopic gel phase. The insoluble component is then washed (Soxhlet) with chloroform for 72 h in order to extract the soluble fraction. IR spectroscopy experiments show that plurifunctional and octylthiophene units are both present in the soluble fraction. Moreover, GPC experiments reveal the presence of large clusters in the soluble fraction. Their molecular weights increase upon decreasing $R_i$ toward the critical value $R_{ic}$, as is expected within a percolation process. The resulting insoluble part is weighted and yields the gel fraction, *G*. When immersing the gels in several apolar solvents, swelling occurs. The equilibrium swelling ratio, *Q*, defined as the volume ratio of the gel swollen over dry gel is measured from weighing the gel after immersion in $CHCl_3$ for 2 days. Values of *G* and *Q* are reported for all studied networks in Table 1. NMR experiments have been performed using a Bruker pulse spectrometer MSL 100 operating at 60 MHz. All relaxation functions are measured by using a Carr−Purcell spin-echo sequence. Pseudosolid echoes which disclose the physical

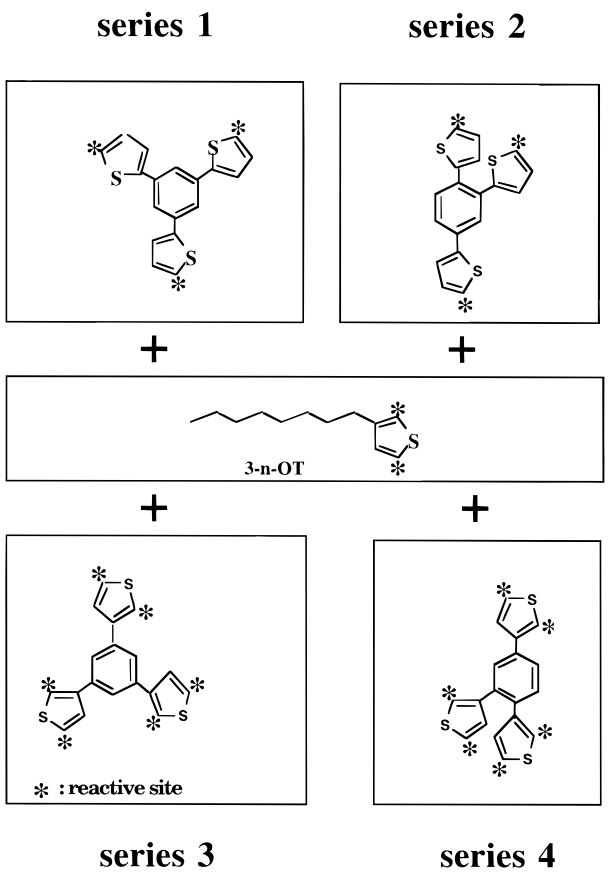


**Figure 1.** Trithienylbenzene units used to form the four gel series by copolymerization.

**Table 1**

| series | $R_i$ | *G* | *Q* | $\chi_c$ (mm$^{-1}$) |
|---|---|---|---|---|
| series **1** ($f = 3$) | 1/10 | 0.87 | | $5.78 \times 10^{-3}$ |
| | 1/15 | 0.89 | 5.8 | $3.9 \times 10^{-3}$ |
| | 1/30 | 0.77 | | $2.59 \times 10^{-3}$ |
| | 1/50 | 0.75 | 5.7 | $2.2 \times 10^{-3}$ |
| | 1/100 | 0.7 | | |
| | 1/100 | 0.63 | 10 | $1.53 \times 10^{-3}$ |
| | 1/100 | 0.61 | | |
| | 1/200 | 0.48 | 15.1 | $1.3 \times 10^{-3}$ |
| | 1/200 | 0.52 | 11 | $1.31 \times 10^{-3}$ |
| | 1/500 | 0.24 | 22.7 | $1.14 \times 10^{-3}$ |
| series **2** ($f = 6$) | 1/12 | 0.9 | | |
| | 1/200 | 0.71 | 9.6 | $1.26 \times 10^{-3}$ |
| | 1/400 | 0.47 | 11 | $1.19 \times 10^{-3}$ |
| | 1/1000 | 0.26 | 16.1 | $1.55 \times 10^{-3}$ |
| series **3** ($f = 3$) | 1/5 | 0.87 | | |
| | 1/100 | 0.39 | 17.4 | $1.46 \times 10^{-3}$ |
| | 1/500 | 0 | | |
| series **4** ($f = 6$) | 1/12 | 0.86 | 5.4 | $3.4 \times 10^{-3}$ |
| | 1/200 | 0.39 | 17.8 | $1.52 \times 10^{-3}$ |
| | 1/400 | 0.23 | 27.3 | $1.08 \times 10^{-3}$ |
| | 1/1000 | 0 | | |

mechanisms of the relaxation of the transverse magnetization (dipole−dipole interaction) are formed using the sequence $(\pi/2)_y-\tau/2-(\pi)_y-\tau/2-(\pi/2)_{-x}-\tau_1/2-(\pi)_y-\tau_1-(\pi)_{-y}-\tau_1-(\pi)_{-y}-\tau_1-(\pi)_y$. Some paramagnetic iron ions may still be present in these systems, due to a nonexhaustive dedoping in methanol. However, the paramagnetic interactions which would induce a fast relaxation process are eliminated by using Carr−Purcell spin echoes.

## III. Principle of the Physical Approach

Gel properties have been extensively studied for about half a century. It is commonly accepted from the original theories of rubber elasticity that the structural properties of gels which have a well-connected structure

(networks prepared far above the gel point) can be described to a large extent in terms of a single length scale. This correlation length, namely, the mesh size, corresponds to the average strand connecting first-neighbor cross-links along the network. In the following $N_{av}$ will denote the number of skeletal bonds of this average strand. This description does not apply to networks which present a loose, poorly connected structure, i.e., networks synthesized near the gel point. Such systems are usually well-described within the framework of percolation,[37,38] applied either in its critical[39] or in its mean-field Flory−Stockmayer[40,41] version. In the percolation model all characteristic quantities like, for instance, the gel fraction or the mesh size can be expressed close to the threshold of percolation as functions of the distance to the critical point, $\epsilon$. The structural state of gelation is characterized in this case by the sole variable $\epsilon$.

In this section after having recalled the percolation theory applied to the sol−gel transition, we assume that the mean-field framework is valid to calculate the structural relevant parameters of POT systems: $\epsilon$ for gels close to the gel point and $N_{av}$ for networks far above the gel point.

**III.1. Loose Gels: Sol−Gel Transition.** The synthesis of networks from a mixture of plurifunctional monomeric units with a variable concentration of bifunctional units is a widespread method. As the reaction among the units proceeds, the size of the formed macromolecules increases. When the extent of the reaction exceeds a certain finite value, a macroscopic cluster emerges. In the immediate vicinity of the threshold the networks have a very large mesh size, which decreases as the reaction goes on. The gel formation is analogous to a percolation process. The three-dimensional percolation view of gelation gives evidence for the variable $\epsilon = (p - p_c)/p_c$ where $p$ is the probability that one chain segment is formed between two plurifunctional units and $p_c$ is the value of $p$ at the threshold.

In POT gels, plurifunctional units are the trithienylbenzene units. They are linked together by linear poly(octylthiophene) segments. It is considered, at the simplest level of approximation, that there is only one variety of functional groups, A, capable of undergoing dimerization. These functional groups are located on the various trithienylbenzene units and on octylthiophene units. The fraction, $\rho$, of reactive groups A which belong to cross-linking units is

$$\rho = \frac{R_i f}{R_i f + 2(1 - R_i)} \tag{1}$$

**(i) Branching Probability.** The calculation of the branching probability $p$ is easily carried out when it is assumed that all A groups are equally reactive, whatever the moiety on which they are located, and that reaction of one functional group of a given unit (octylthiophene or trithienylbenzene) does not modify the reactivity of other unreacted groups of the same unit. This hypothesis is reasonable for A groups located on octylthiophene or on 1,3,5-trithienylbenzene units (gel series **1** and **2**) but is not valid for A groups located on 1,2,4-trithienylbenzene units, as will be shown later. Indeed, in this latter case, there are always at least two functional groups which are very close to each other so that the reaction of one of these groups may significantly decrease the reactivity of the other one. In this work, we will limit our calculation of $p$ and $\epsilon$ to the case of gels of series **1** and **2**.

Let $\pi$ denote the ratio of reacted A groups to all A groups; $\pi$ is the probability that any particular functional group has undergone reaction. According to the description of gelation processes proposed by Flory,[40] the branching probability, $p$, is readily expressed as

$$p = \sum_{i=0}^{\infty} [\pi(1 - \rho)]^i \pi\rho \tag{2}$$

which reduces to

$$p = \frac{\pi\rho}{1 - \pi(1 - \rho)} \tag{3}$$

**(ii) Variable of Gelation.** The variable $\epsilon$, equal to $(p - p_c)/p_c$ is expressed for gel series **1** and **2** from eqs 1 and 3 as

$$\epsilon = \frac{\left(\frac{f}{2(1-\pi)}\left(\frac{\pi}{p_c} - 1\right) + 1\right)R_i - 1}{\left(\frac{f}{2(1-\pi)} - 1\right)R_i + 1} \tag{4}$$

The term $(f/[2(1 - \pi)])/(\pi/p_c - 1) + 1)$ can be defined as the inverse, $R_{ic}^{-1}$, of the value of $R_i$ at the threshold of gelation. The order of magnitude of $R_{ic}$ of gels series **1** and **2** will be experimentally shown to be $10^{-3}$ so that $(f/[2(1 - \pi)](\pi/p_c - 1) + 1)$ can be reduced to $(f/[2(1 - \pi)](\pi/p_c - 1)$. We assume that the parameter $\pi$ is a constant close to 1 since the chemical reaction is pursued until its term. Therefore, considering that $1/(1 - \pi) \gg 1$, eq 4 can be expressed in a simpler form using the reduced variable $x$ as

$$\epsilon(x) = \frac{x\left(\frac{\pi}{\pi_c} - 1\right) - 1}{x + 1} \tag{5}$$

$$x = \frac{fR_i}{2(1 - \pi)} \tag{5'}$$

It must be noted that the parameter $p_c$ depends on local mechanisms of network formation. Current estimates of $p_c$ for a regular three-dimensional lattice range from 0.198 (FCC) to 0.2488 (cubic) to 0.3886 (diamond) and depend on the coordination number of the percolation lattice. However, as POT gelation results from a complex synthesis, no regular lattice on which gelation proceeds can be defined. Therefore, for the sake of simplicity we will consider $p_c$ as being constant[42] for gel series **1** and **2**. The variable $\epsilon$ then depends only on the variable $x$, and the physical quantities associated with $\epsilon$ are then predicted to be solely a function of $x$. Consequently, master curves of variations of these quantities must be obtained versus $fR_i$ for loose gels of series **1** and **2**.

**III.2. From Loose to Tight Gels: Structural Mesh Size.** The collective behavior of the structural segments which can be associated with the gel mesh size is known to govern most of the mechanisms of deformation of the networks. The gel mesh size characterizes the distance above which one can consider that the gel has a well-connected structure. It is infinite at the gel point, and the associated structural segment, extended to the whole gel, is large and branched. In POT gel, it is made of several linear segments linked

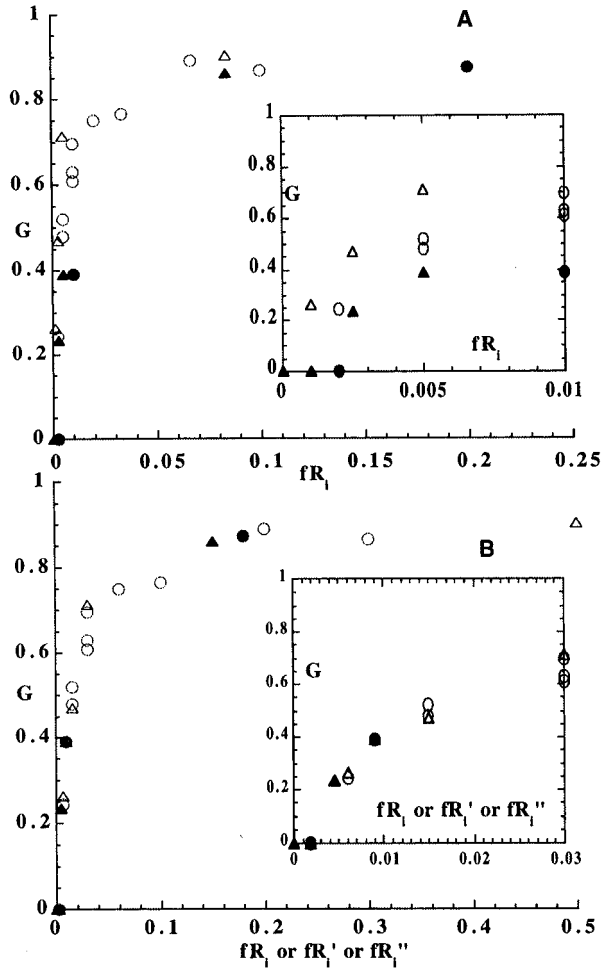


**Figure 2.** (A) Variations of the gel fraction versus the cross-link concentration (B) Variations of the gel fraction versus the following reduced variables: $fR_i$ for series **1** and **2**, $fR_i'$ for series **3**, and $fR_i''$ for series **4**. A master curve is observed. Gel series: **1** (○), **2** (△), **3** (●), and **4** (▲).

together by cross-links. Above the gel point the mesh size, controlled by the variable $\epsilon$, progressively decreases. Farther from the threshold, the network structure is tight and well-connected at all length scales. The percolation model is no longer relevant. The theory of rubber elasticity may apply: the characteristic segment is the linear segment between two adjacent cross-links. Its segmental contour length $N_{av}$ can be derived from the stoichiometry, $N_{av} = 2/fR_i$. It must be stressed that $N_{av}$ does not diverge at the threshold of gelation as it should. Its value is $2/fR_{ic}$. It is also worth noting that the two relevant structural parameters of loose gels and tight gels, respectively $\epsilon$ and $N_{av}$, are both functions of the product $fR_i$. This quantity is therefore predicted to be the relevant variable of description of POT gels.

## IV. Gel Fraction

The gel fraction, $G$, measures the proportion of clusters attached to the gel phase. This quantity direcly reflects the state of connectivity of the network. It is a natural function of the variable $\epsilon$. $G$ is equal to 0 as long as only finite clusters exist in the system. It is equal to 1 whenever all monomers are attached to one another. Experimental values of $G$ are reported in Figure 2A as a function of $R_i$. Two systems are totally soluble in $CHCl_3$, as indicated in Table 1: they are composed of clusters below the gel point. As expected, $R_i$ is not a relevant variable since four distinct curves are observed corresponding to the four gel series synthesized with different trithienylbenzene units. It is worth noting that the experimental curves of gel series **3** and **4** are not identical with curves of series **1** and **2**, respectively. This shows that the corresponding gel states are not the same for a given value of $R_i$, although the theoretical functionality of the compared gels are identical. This result supports the idea that the pertinent variable $\epsilon$ cannot be described by eq 4 for gel series **3** and **4**, due to the decrease of the reactivity of A groups of 1,2,4-trithienylbenzene units located nearby already reacted neighboring A groups.

**IV.1. Master Curve.** Variations of $G$ versus the reduced variable $fR_i$ are shown in Figure 2B. A single master curve is obtained, as predicted by eq 5. Empirical expansion factors, $\phi_3$ and $\phi_4$, are applied to the $fR_i$ scale of curves drawn for gel series **3** and **4**, respectively, in order to superpose these curves to the previous one (Figure 2B). For the gel series **3**, $f = 3$ and $\phi_3 = 0.3$, and for the gel series **4**, $f = 6$ and $\phi_4 = 0.3$. These two expansion factors are *ad hoc* scale parameters which allow one to identify the gelation state of gels of series **3** and **4** by associating with a given gel its effective reduced variable $fR_i' = f\phi_3 R_i$ or $fR_i'' = f\phi_4 R_i$. For the gel series **3**, $\phi_3$ may be seen as a measure of the decrease of reactivity of 1,2,4-trithienylbenzene units compared to 1,3,5-trithienylbenzene units. The probability that the three functional A groups have reacted is reduced so that the cross-link density has to be rescaled to account for the fact that approximately 30% of 1,2,4-trithienylbenzene units act as effective cross-links.

The value of $fR_{ic}$ is approximately estimated by extrapolating $R_i$ at the maximal value for which the gel fraction equals 0. From Figure 2B, this value is found to lie in the range $10^{-3}-5 \times 10^{-3}$; i.e. $R_{ic}$ are on the order of $3 \times 10^{-4}-1.6 \times 10^{-3}$ and $1.7 \times 10^{-4}-8.3 \times 10^{-4}$ for gel series **1** and **2**, respectively.

It has to be noted that, for values of $fR_i$ higher than 0.15, $G$ remains constant since most finite clusters have been attached to the gel. $G$ is not a quantity able to discriminate the structural state of highly cross-linked gels. The percolation model is not relevant for the description of these latter systems.

**IV.2. Variable of Gelation.** We would like to have an estimate of the parameters of eq 5. To do this, we propose to calculate the variations of $\epsilon$ with the cross-link concentration $R_i$ in order to determine values of $p_c$ and $\pi$ and to check whether they are realistic or not. Indeed, the position of the gel point $p_c$ depends on the microscopic local mechanisms of gel formation which are unknown and $\pi$ cannot be easily measured. The law $\epsilon(R_i)$ can be obtained by assigning to each experimental value of $G(R_i)$ the corresponding theoretical value of $\epsilon$ determined from a theoretical curve of variations of $G(\epsilon)$. However, no analytical description of the curve $G(\epsilon)$ exists beyond the scaling domain, except for the very particular case of percolation on a Bethe lattice (i.e., when no loop is formed in the network). Approximate descriptions of $G(\epsilon)$ are, nevertheless, available whose domains of validity depend on how far the gel is from the gelation point.[39] Let us call $n_s$ the distribution function of clusters made of $s$ monomers. Close to the percolation threshold, $n_s$ is described as

$$n_s \propto s^{-\tau} f(-\epsilon^{1/\sigma} s) \qquad (6)$$

where $f$ is a fast decreasing function. Within the mean-field approximation $\tau = 2.5$, $1/\sigma = 2$, and $f$ is a Gaussian $f(x) = \exp(-cx^2)$.

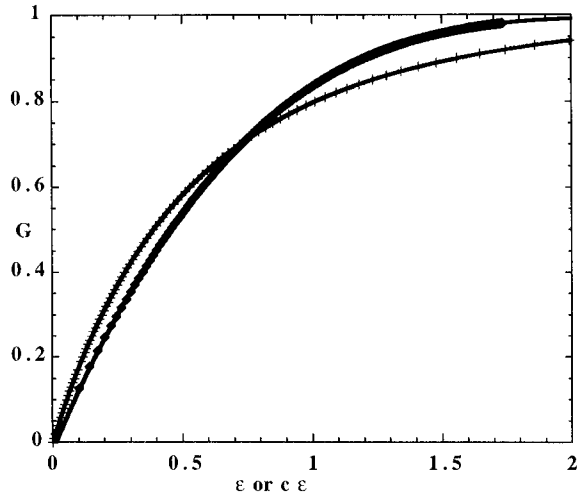


**Figure 3.** Theoretical variations of $G$ versus a quantity proportional to $\epsilon$ derived from eq 7 (◆) and theoretical variations of $G$ versus $\epsilon$ obtained analytically for a Bethe lattice (+). Solid lines: fit by polynomial curves of degree 5.

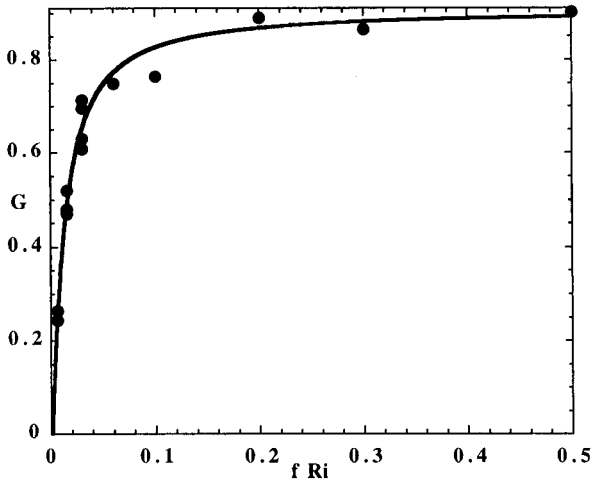


**Figure 4.** Fit (solid line) of the curve of variations of $G$ versus the variable $fR_i$. The fit is performed from eq 7, using the polynomial curve of Figure 3, and from eq 5.

The gel fraction is the ratio of units which are not involved in the formation of finite clusters. It is expressed as

$$G = 1 - \sum_{s=1}^{s=\infty} s n_s \qquad (7)$$

Variations of $G$ versus $\epsilon$ calculated, on the one hand, for the exact solution of percolation on a Bethe lattice[43] and, on the other hand, according to eq 7 with $n_s$ determined from eq 6 using mean-field values are plotted in Figure 3.

These two curves have been fitted by using eq 5 in order to obtain a set of values for the parameters $p_c$, $\pi$, and $c$. Fits obtained from the function $G(\epsilon[fR_i])$ derived from the Bethe lattice are not good. The fits observed from eq 7 have been performed first by fixing $fR_{ic}$, in order to have only two adjustable parameters. Several reasonable values for $fR_{ic}$ have been tested, and the best fits have been obtained for the smallest values of $fR_{ic}$. The fit represented in Figure 4 is obtained with the set of values $fR_{ic} = 1.85 \times 10^{-3}$, $c = 0.11$, and $\pi = 0.99$, which yields the value $p_c = {}^1/_{12}$.

The two functions $G(\epsilon)$ derived from the Bethe lattice and from eq 7 result from simplified approaches of the real percolation process so they are thought to give only an approximate representation of the real shape of the curve $G(\epsilon)$. However, the good quality of the fit observed from eq 7 and the reasonable order of magnitude found for the parameters $\pi$ and $p_c$ support the method of analysis proposed in this work.

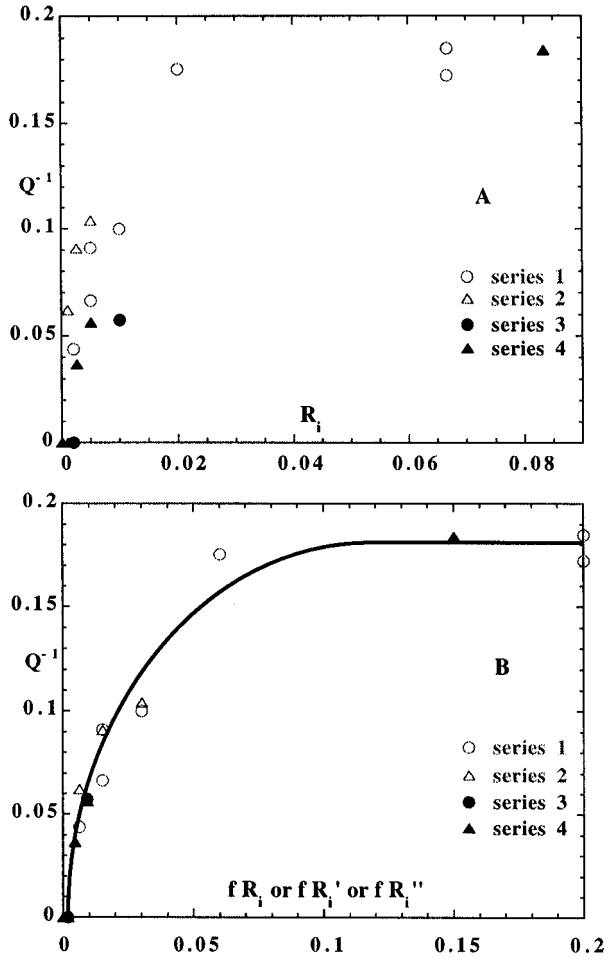


**Figure 5.** (A) Inverse of the swelling ratio versus the cross-link concentration. (B) Inverse of the swelling ratio versus the reduced variables used in Figure 2B: a master curve is observed.

## V. Swelling Ratio

An analysis similar to that used for the gel fraction is applied to the inverse of the swelling ratio. The swelling ratio $Q$ is defined as the ratio of volumes of the gel in the fully swollen and dry states (with the sol fraction removed in each case). Experimental curves of variations of $Q^{-1}$ versus $R_i$ are plotted in Figure 5A: $Q^{-1}$ increases with $R_i$, starting from the value $Q^{-1} = 0$ taken for all systems below the gel point. Four distinct curves are observed corresponding to the four gel series.

**V.1. Master Curve.** $Q^{-1}$ is represented in Figure 5B versus the reduced variable $fR_i$ and versus the empirical variables $fR_{i'}$ and $fR_{i''}$ determined in the previous section. A single master curve is obtained, similar to what was observed for the gel fraction. This result proves that the macroscopic physical quantities $G$ and $Q$ depend on the same variable. Furthermore, in order to confirm this result, experimental variations of $Q^{-1}$ are directly reported as a function of $G$. Experimental points measured on all the gels are found to be located on a single curve, whatever the cross-link density or the nature of cross-linking units (Figure 6).

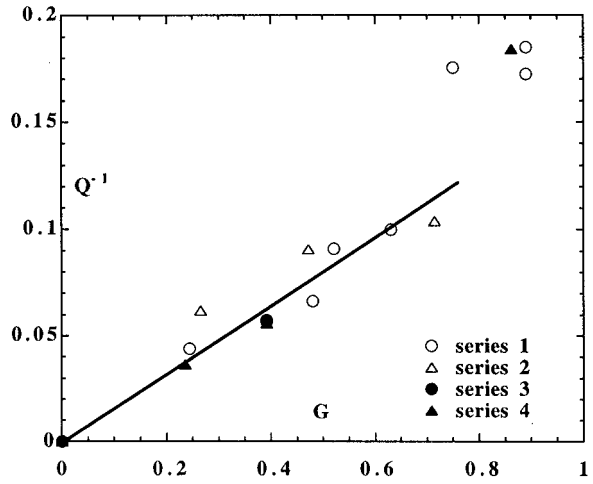


**Figure 6.** Variations of the inverse of the swelling ratio versus the gel fraction.

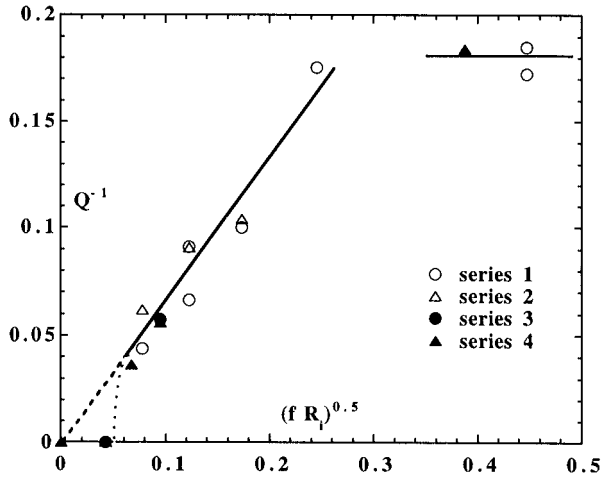


**Figure 7.** Variations of the inverse of the swelling ratio versus the square root of $fR_i$: (- - -) extrapolation of the linear curve to the origin; (···) schematic representation of the variations $Q^{-1}$versus $(fR_i)^{0.5}$ near the gelation point.

**V.2. Statistical Structure: a Packing Condition.** The structural segments which govern the mechanisms of isotropic deformations can be conveniently studied from the observation of fully swollen gels. According to the $c^*$ theorem of de Gennes for network swelling,[37] the statistical structural segments are presumed to be just at the overlap concentration when fully swollen. Thus, in situations where network strands are strongly overlapped in the unswollen state, they must be completely disinterspersed to get to $c^*$ in the swollen state. Let $N$ denote the average degree of polymerization of the statistical structural element, which controls the gel characteristic length $R$ after the swelling has reached its maximum value

$$R \propto N^{\nu} \tag{8}$$

The exponent $\nu$ is $^1/_2$ for dilute branched polymers where screening effects have disappeared or for ideal linear chain segments and 0.588 for linear segments which obey excluded-volume statistics. Then, considering that the gel is a close packing of chain elements of size $N$, disengaged from one another, the inverse of $Q$, i.e., the concentration of the gel, is expressed as

$$Q^{-1} \approx N\omega/R^3 \propto N^{1-3\nu} \tag{9}$$

where $\omega$ is the monomeric volume. Variations of $Q^{-1}$ are represented as a function of $(fR_i)^{1/2}$ in Figure 7. It is clearly seen that $Q^{-1}$ is a linear function of $(fR_i)^{1/2}$ over the range $5 \times 10^{-3} < fR_i < 9 \times 10^{-2}$. This result suggests that, within this range of $fR_i$ values, $N$ is proportional to $N_{av} = 2/fR_i$. The relevant active element of a gel corresponds to the linear segment comprised between adjacent cross-links. The exponent $\nu$ is equal to 0.5, indicating a Gaussian chain statistic which reveals a persistence of screening effects. Such effects have already been mentioned in the literature in the case of swollen vulcanizates[44] but are still not fully understood.

The swollen gel can therefore be pictured as a close packing of Gaussian linear coils sealed together by cross-links. It is worth noting that the swelling phenomenom is mainly due to the disengagement of coils which are strongly overlapped in the dry state. Indeed, if $R_G$ is the radius of gyration of a Gaussian coil of degree of polymerization $N$, the volume $R_G{}^3$ statistically occupied by one macromolecule in the dry state is also occupied by $R_G{}^3/N\omega$, i.e., $N^{1/2}$ other overlapping molecules in the dry state. At the maximum swelling, each molecule occupies alone a volume $R_G{}^3$ so that the swelling ratio is proportional to the ratio $N^{1/2}$.

A plateau is observed at $Q = 6$ for systems prepared with values of $fR_i$ greater than $9 \times 10^{-2}$. This plateau can be explained in the following way. High values of $fR_i$ correspond to short average spacings between adjacent cross-links ($N_{av} < 20$), shorter than the persistence length of POT chains which is the characteristic distance within which the polymer backbone maintains its direction. Therefore, the chain segments between two neighboring cross-links behave like semirigid strands which undergo weak conformational fluctuations and which occupy small statistical volumes. Correspondingly, the degree of overlapping of the strands in the dry state becomes negligible and no significant chain disinterspersion can occur during swelling. As a consequence, the swelling ratio is constant, independent of the chain segment length. It probably reflects only an increase of the free volume of the gel and an enhancement of conformational fluctuations due to the presence of solvent.

Two comments can be addressed concerning the swelling behavior of POT gels. First, the maximum swelling is controlled by the linear segments between cross-links, even for gels synthesized not far from the percolation threshold ($G < 0.7$). This result proves that the $\epsilon$-domain for which the active structural segment is branched is very small. Within this domain a deviation from the linear law $Q^{-1} \propto (fR_i)^{1/2}$ must be observed to reach the limit $Q^{-1} = 0$ at the value $R_i = R_{ic}$. However, this domain has not been detected experimentally since the gels we have synthesized are too highly cross-linked. Second, as $Q$ remains constant since for values of $fR_i$ higher than $9 \times 10^{-2}$ it cannot constitute an experimental quantity able to discriminate the structural state of highly cross-linked gels.

## VI. Statistical Structure of Dry States: NMR Approach

In this section we briefly recall the principle of the NMR approach and we discuss the physical state of dry networks at a temperature higher than the melting temperature of the chain segments. It has been now well established that the nuclear magnetic relaxation of protons linked on polymer gels can reveal the statistical structure of gels.[45]

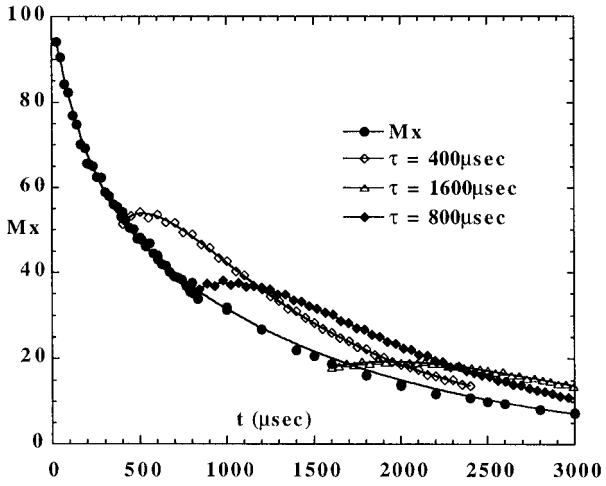


**Figure 8.** Relaxation of the transverse magnetization of a gel of series **1**, $R_i = 1/100$. Pseudosolid echoes originated at several times $\tau$ are displayed to show that the mechanisms of relaxation are governed by dipolar interactions.

**VI.1. Principle of the NMR Approach.** The principle of the NMR approach relies on the observation of the transverse magnetic relaxation of spins of protons located on polymer chains. It is based on the significant reduction of dipole−dipole interactions existing among nuclear spins induced by the fast molecular diffusional motions of monomeric units which occur above $T_g$. The conformational fluctuation of a chain segment defined by two consecutive cross-links is, however, restricted and nonisotropic because of the presence of the nodes at its ends. Dipolar interactions are therefore not averaged to zero. The residual dipolar interaction governs the relaxation of the transverse magnetization of gels. It is sensitive to the reduction of entropy affecting the chain segments caused by the presence of cross-links.

The identification of the mechanisms of relaxation of the magnetization is necessary to determine the nature of the information provided by NMR observations. This can be done easily by the observation of pseudosolid echoes on the NMR signal.[45] Such echoes are formed only when the relaxation of the transverse magnetic relaxation is governed by pure residual dipolar interactions. A typical relaxation curve observed from protons attached to the polymer is drawn from Carr−Purcell spin echoes, in Figure 8. Pseudosolid spin echoes are well-defined. The presence of pseudosolid spin echoes proves that the relaxation mechanism is mainly due to residual dipole−dipole interactions of protons. Therefore, the relaxation curves are only sensitive to the degree of anisotropy of rotations of monomeric units.

It is worth noting that the great majority of protons are located on the alkyl lateral chains. However, the presence of pseudosolid spin echoes proves that by restricting the fluctuation motions of the skeleton chains, the cross-links also strongly hinder the molecular motions of the alkyl lateral chains. The NMR relaxation of protons located on the lateral chains of a given chain segment comprised between two topological constraints therefore reflects the residual dipolar interaction of the considered chain segment of contour length $N$. It is expressed as[44]

$$\langle H_D(\mathbf{r}_N,N)\rangle = (3\cos^2\theta_N - 1)\frac{\mathbf{r}_N^{\,2}}{\langle \mathbf{r}_N^{\,2}\rangle^2} a^2 \Lambda H_D^{\,0} \quad (10)$$

where $H_D^0$ is the dipole−dipole interaction which should be observed along one chain segment in the glassy state, $a$ is the skeletal bond length, $\mathbf{r}_N$ is the nonzero average end-to-end vector of the chain segment, $\theta_N$ is the angle between the end-to-end vector $\mathbf{r}_N$ and the steady magnetic field, and $\langle \mathbf{r}_N^2\rangle$ is the mean-square end-to-end distance of a segment of size $N$; it is proportional to $N$ for a Gaussian chain; $\Lambda$ accounts for angular correlations among three neighboring skeletal bonds of the segment.

The relaxation function assigned to the chain segment is written as

$$M_x(\mathbf{r}_N,N)(t) = \mathrm{Tr}\{e^{i\langle HD(\mathbf{r}_N,N)\rangle t} M_x e^{-i\langle HD(\mathbf{r}_N,N)\rangle t} M_x\}/\mathrm{Tr}\{M_x^{\,2}\} \quad (11)$$

The relaxation function of the whole sample, $M_x(t)$, is the average of $M_x(\mathbf{r}_N,N)$ over all network chain segments.

**VI.2. NMR Structural Parameter.** A specific method of analysis of relaxation curves has been recently developed[44] by considering the two easily computable integrals

$$\phi_1 = \int_0^\infty (\sqrt{t})^{-1} M_x(t)\, dt \quad (12)$$

$$\phi_3 = \int_0^\infty (\sqrt{t})^{-1} \frac{dM_x(t)}{dt}\, dt \quad (13)$$

Then, we define the ratio $\chi_c = \phi_3/\phi_1$, equal to

$$\chi_c = A\Lambda\langle N\rangle^{-2n} \quad (14)$$

where $\langle N\rangle$ is the mean contour length of the structural chain segments and $A$ is a constant. If the structural chain segment is the segment comprised between two successive cross-links, $\langle N\rangle = N_{av}$.

Therefore, $\chi_c$ is the NMR structural parameter which reflects the size of the gel constitutive segments. Equation 14 shows that $\chi_c$ must be a simple function of the average number of skeletal bonds which form one characteristic network chain segment.

**VI.3. Variations of the Segmental Length.** The relaxation functions are recorded on dry extracted gels above the fusion temperature at 150 °C. The evolution of the structural parameter $\chi_c$ is reported as a function of the reduced variable $fR_i$ in Figure 9. A linear variation is observed

$$\chi_c = \chi_c(0) + \lambda f R_i \quad (15)$$

with experimental values $\lambda = 0.0148$ and $\chi_c(0) = 0.001\,09\ \mu s^{-1}$.

The value of $\chi_c(0)$ reflects the state of constraints extrapolated for a cross-link density equal to 0 (i.e., linear molten POT chains). The value of $\chi_c$ observed in polymer melts composed of long entangled chains is currently associated with the temporary entanglement network perceived by mechanical experiments and by NMR when the lifetime of the network is long compared to the NMR time scale. In our case, the value of $\chi_c(0)$ is extrapolated from values of the cross-link density much smaller than the density of entanglements. We therefore consider that $\chi_c(0)$ reflects the entanglement temporary network trapped in the gels because of the presence of permanent cross-links. The observed linear law (15) suggests that entanglements are defined independently from the cross-link density (probably as long

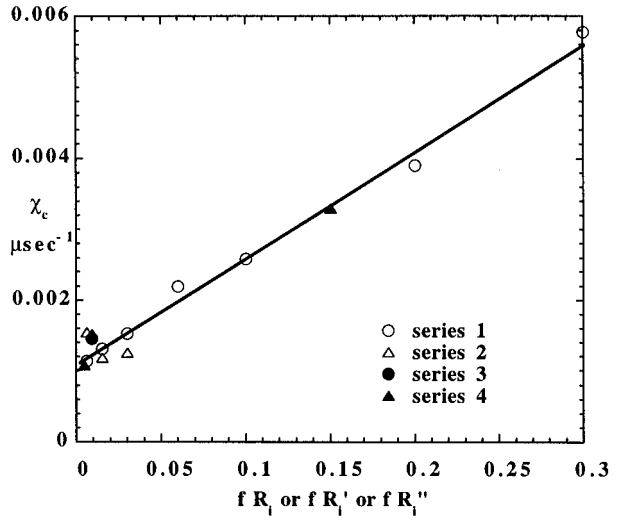


**Figure 9.** Linear variations of the structural NMR parameter, $\chi_c$, versus the reduced variables used in Figure 2B.

as the cross-link density keeps smaller than the density of entanglements). This linear law reveals that the effects of cross-linking upon the NMR behavior are additive. Let $\nu_e$ denote the density of entanglements, $\nu_e = K_1/N_e$, where $N_e$ is the number of skeletal bonds between entanglements and $K_1$ is a constant. The cross-link density is $\nu_c = K_2\, fR_i$, where $K_2$ is a constant. The total concentration of topological constraints per skeletal bond is equal to $\nu_t = \nu_e + \nu_c = K_1/N_e + K_2\, fR_i$ and is proportional to the inverse of the average segmental length between constraints (either entanglements or cross-links). Therefore, according to eq 14, $\chi_c$ can be written as $\chi_c = A\Lambda(K_1/N_e + K_2 fR_i)$, where the chains are supposed to be Gaussian ($\nu = 0.5$). This relation describes the experimental linear curve given by eq 15 with $\chi_c(0) = A\Lambda K_1/N_e$ and $\lambda = A\Lambda K_2$.

This result proves that the structural segment detected by NMR is the linear segment defined by adjacent topological constraints (entanglement or covalent junction).

Furthermore, it has to be noted that, contrary to the behaviors of $G$ and $Q^{-1}$, no plateau is reached for highly cross-linked gels. The NMR approach perceives the progressive increase of cross-link density during the whole process of gelation. It confirms that the structure of POT networks progressively changes with the cross-link density up to highly cross-linked gels.

## VII. Statistical Structure: Summary

We have studied the structural properties of POT gels from three quantities: the gel fraction, the equilibrium swelling ratio, and the $^1$H transverse relaxation rate. The quantities $G$, $Q$, and $\chi_c$ probe specific and complementary gel structural properties over an increasing range of $fR_i$ values.

The gel fraction describes the state of connectivity of loose networks. It is directly related to the gel mesh size. We have established a master curve of variations of $G$ versus the reduced variable which characterizes the distance to the gel point, $fR_i$. This result demonstrates that the percolation model is pertinent to describe the state of connectivity of loose POT gels. However, for values of $fR_i$ greater than 0.15, $G$ is constant and close to unity. This indicates that the mesh size of highly cross-linked systems is short, i.e., that these networks have a well-connected structure and that $G$ is no longer a pertinent quantity.

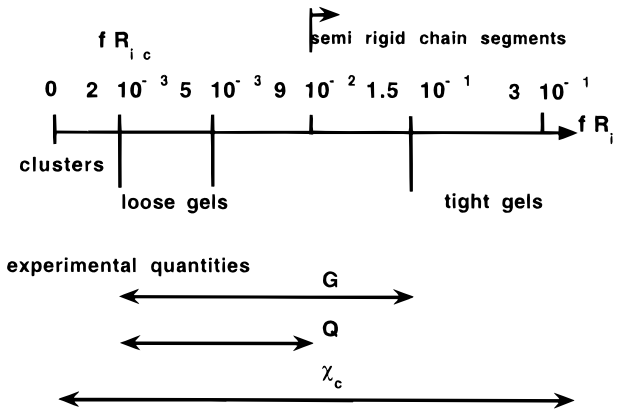


**Figure 10.** Schematic behavior of POT gels along the $fR_i$ scale.

The study of the equilibrium swelling of these gels has allowed us to describe their mechanisms of isotropic deformation induced by osmotic pressure. In the range $5 \times 10^{-3} < fR_i < 9 \times 10^{-2}$, we have shown that the swelling mechanism is a segmental disengagement process which is governed by the linear strands between cross-links. Closer to $fR_{ic}$, the swelling active segment must be large and branched: it varies like the mesh size and extends over the whole gel at the percolation threshold as $Q$ tends to infinity. However, this $fR_i$ domain of POT gels is quite narrow ($fR_{ic} < fR_i < 0.005$) and has not been observed, probably due to the narrowness of the domain and also because loose networks are fragile and hard to handle. Furthermore, the swelling ratio reaches a plateau when $fR_i > 9 \times 10^{-2}$ and can therefore not be used to discriminate the structure of highly cross-linked systems.

The NMR parameter $\chi_c$ reveals the state of deformation of dry networks in the absence of external applied force. Segmental deformation is induced by the presence of topological constraints. The statistical segment which corresponds to the NMR correlation domain is the linear segment comprised between either trapped entanglements or cross-links. The parameter $\chi_c$ is expected to be closely related to the elasticity modulus.

The two latter approaches, swelling (macroscopic information) and NMR (microscopic information), disclose that the mechanisms of deformation of these gels are governed by the segments between cross-links (parameter $fR_i$) as long as the gels are not "very close" to the gel point. However, the role of trapped entanglements in the swelling process has not been evidenced, probably because they can slip along the chains in swollen gels.

Finally, it clearly appears from the three measured physical quantities that the structural parameter $\chi_c$ is the only one that can discriminate the various network structures over the whole range explored $0 < fR_i < 0.3$. This result is schematically illustrated in Figure 10.

## VIII. Conclusion

We have reported the first study of the statistical structure of well-defined fully conjugated covalent gels. The ensemble of the results we have obtained shows that the method of synthesis of these networks is well controlled since the quantities we have measured vary smoothly with the cross-link density of the gels.

This approach has demonstrated that the gel statistical structure changes monotonously with the cross-link concentration. The statistical structure of different gels is the same as long as the product $fR_i$ or $fR_i'$ or $fR_i''$ is

the same. Moreover, a further insight into the statistical properties has indicated that the structural active element of these networks is the segment comprised between cross-links.

It is of interest to mention the results of Pepin-Donat *et al.*,[36] who have found that the highest conductivity and the largest size of the conducting clusters and of the crystalline domains[46] of these gels have been obtained for systems of intermediate cross-linking concentration ($R_i = 1/100$). In light of our study these optimized properties cannot be directly related to the gel statistical structure which is a monotonous function of the cross-link concentration. This peak of conductivity is more likely induced by the structure of the crystallized systems. We believe that the structural changes which accompany the increase of the cross-link density give the most favorable crystalline structure for the gel $R_i = 1/100$ at room tempeature. A detailed study of the crystalline behavior of these gels is in progress at the moment.

## References and Notes


(1) Shiguro, T.; Kaneko, H.; Nogami, Y.; Ishimoto, H.; Nishiyama, H.; Tsukamoto, J.; Takahashi, A.; Yamaura, M.; Hagiwara, T.; Sato, K. *Phys. Rev. Lett.* **1992**, *69*, 660.
(2) Ishiguro, T.; Kaneko, H.; Pouget, J. P.; Tsukamoto, J. *Synth. Met.* **1995**, *69*, 37.
(3) Reghu, M.; Yoon, C. O.; Moses, D.; Heeger, A. J.; Cao, Y. *Phys. Rev. B* **1993**, *48*, 17685.
(4) Yoon, C. O.; Reghu, M.; Moses, D.; Heeger, A. J. *Phys. Rev. B* **1994**, *49*, 10851.
(5) MacCullough, R. D.; Tristam-Nagle, S.; Williams, S. P.; Lowe, R. D.; Jayaraman, M. *J. Am. Chem. Soc.* **1993**, *115*, 4910.
(6) Oh, E. J.; Min, Y.; Manohar, S. K.; Macdiarmid, A. G.; Epstein, A. J. *Abstr. Am. Phys. Soc. Meet.* **1992**, March 19, No. M30-8.
(7) Tzou, K. T.; Gregory, R. V. *Polym. Prepr.* **1994**, *35*, 245.
(8) Tzou, K.T.; Gregory, R. V. *Synth. Met.* **1995**, *69*, 109.
(9) Gettinger, C. L.; Heeger, A. J.; Pine, D. J.; Cao, Y. *Synth. Met.* **1995**, *74*, 81.
(10) Laasko, J.; Järvinen, H. *Synth. Met.* **1993**, *55−57*, 1204.
(11) Tzou, K.-T.; Gregory, R. V. *Synth. Met.* **1993**, *55−57*, 983.
(12) Oka, O.; Morita, S.; Yoshino, K. *Jpn. J. Appl. Phys.* **1990**, *29*, L 679.
(13) MacDiarmid, A. G.; Tang, X. U.S. Patent 5,147,913, Sept 15, 1992.
(14) Yoshino, K.; Nakao, K.; Sugimoto, R. *Jpn. J. Appl. Phys.* **1989**, *28*, L490.
(15) Yoshino, K.; Nakao, K.; Onoda, M. *Jpn. J. Appl. Phys.* **1989**, *28*, L682.
(16) Yoshino, K.; Nakao, K.; Morita, S. *Jpn. J. Appl. Phys.* **1989**, *28*, L2027.
(17) Yoshino, K.; Nakao, K.; Onoda, M.; Sugimoto, R. *Solid State Commun.* **1989**, *70*, 609.
(18) Yoshino, K.; Nakao, K.; Onoda, M. *Jpn. J. Appl. Phys.* **1989**, *28* (6), L1032.
(19) Yoshino, K.; Nakao, K.; Onoda, M. *J. Phys.: Condens. Matter* **1990**, *2*, 2857.
(20) Morita, S.; Kawai, T.; Yoshino, K. *Technol. Rep. Osaka Univ.* **1991**, *41*, 99.
(21) Morita, S.; Kawai, T.; Onoda, M.; Yoshino, K. *Solid State Commun.* **1991**, *77* (10), 807.
(22) Morita, S.; Kawai, T.; Yoshino, K. *J. Appl. Phys.* **1991**, *69*, 4445.
(23) Yoshino, K.; Morita, S.; Nakao, K. *Synth. Met.* **1991**, *41−43*, 1039.
(24) Morita, S.; Shakuda, S.; Sugimoto, R.-I. *Jpn. J. Appl. Phys.*. **1992**, *31*, L1563.
(25) Yoshino, K.; Morita, S.; Sugimoto, R. *Synth. Met.* **1992**, *49−50*, 491.
(26) Yoshino, K.; Morita, S.; Uchida, M.; Muro, K.; Kawai, T.; Ohmori, Y. *Synth. Met.* **1993**, *55−57*, 28.
(27) Morita, S.; Shakuda, S.; Sugimoto, R.; Yoshino, K. *Synth. Met.* **1993**, *55−57*, 1182.
(28) Taka, T.; Jylhä, O.; Root, A.; Silvasti, E.; Österholm, H. *Synth. Met.* **1993**, *55−57*, 414.
(29) Morita, S.; Shakuda, S.; Kawai, T.; Yoshino, K. *Synth. Met.* **1995**, *71*, 2231.
(30) Pei, Q.; Inganäs, O. *Synth. Met.* **1993**, *55−57*, 3724.
(31) Shikawa, S.; Ito, M.; Okamoto, M.; Nakamori, T. *Polymer* **1996**, *37*, 3763.
(32) Fizazi, A.; Moulton, J.; Pakbaz, K.; Rughooputh, S. D. D. V.; Smith, P.; Heeger, A. J. *Phys. Rev. Lett.* **1990**, *64* (18), 2180.
(33) De Gennes. P. G. *C. R. Acad. Sci., Paris* **1986**, *302*, Série II, No.° 1, 1.
(34) Rebourt, E.; Pépin-Donat, B.; Dinh, E. *Polymer* **1995**, *36* (2), 399.
(35) Rebourt, E.; Pépin-Donat, B.; Dinh, E. *Synth. Met.* **1995**, *69*, 293.
(36) Sixou, B.; Pépin-Donat, B.; Nechtschein, M. *Polymer*, accepted for publication.
(37) de Gennes, P. G. *Scaling concepts in polymer physics*; Cornell University Press: Ithaca, NY, 1979.
(38) Stauffer, D; Coniglio, A; Adam, M. *Adv. Polym. Phys.* **1982**, *44*, 103.
(39) Stauffer, D.; Aharony, A. *Introduction to percolation theory*, 2nd ed.; Taylor and Francis: London, 1985.
(40) Flory, P. J. *Principles of polymer chemistry*; Cornell University Press: Ithaca, NY, 1953.
(41) Stockmayer, W. H. *J. Chem. Phys.* **1943**, *11*, 45.
(42) The mechanisms of network formation are expected to be the same, whatever the nature of the trithienylbenzenes. In particular, stacking of the rigid oxidized crosslinks may occur at the proximity of $FeCl_3$ ions, giving rise to the formation of small aggregates which may act as effective gel nodes. However, these effective nodes are not thought to depend much on the nature of the 1,3,5-trithienylbenzene units so that $p_c$ is taken as a constant.
(43) The equation which gives $G(\epsilon)$ variations is $1 - (1 - G)^{1/f} = p[1 - (1 - G)^{(f-1)/f}]$, with $\epsilon = p(f - 1) - 1$. It is slowly dependent on $f$ only for small $f$ values and is represented in Figure 3 for large $f$ values.
(44) Cohen Addad, J. P. *Physical properties of polymeric gels*; Cohen Addad, J. P., Ed.; John Wiley & Sons: New York, 1996.
(45) Cohen Addad, J. P. *NMR and Fractal properties of polymeric liquids and gels*; Pergamon Press: New York, 1992.
(46) Pepin-Donat, B.; Sixou, B.; Rebourt, E. Proceedings of the Europhysics Conference on gels Balatonzeplak, Hungary, Sept 25−29, 1995.


MA961909Y